Memorias del Congreso Nacional de Control Automático
ISSN: 2594-2492

Robust estimation and control of a batch Hydrothermal Carbonization reactor

S. Andrade * **J. Alvarez** ** **L. Alvarez-Icaza** *** **L. Samarti** ****

* *Instituto de Ingeniería, Universidad Nacional Autónoma de México, CDMX, México (e-mail: sandradeb@ iingen.unam.mx)*
** *Departamento de Procesos e Hidráulica, Universidad Autónoma Metropolitana-Iztapalapa, CDMX, México (e-mail: jac@xanum.uam.mx)*
*** *Instituto de Ingeniería, Universidad Nacional Autónoma de México, CDMX, México (e-mail: alvar@ pumas.unam.mx)*
**** *Departamento de Procesos e Hidráulica, Universidad Autónoma Metropolitana-Iztapalapa, CDMX, México (e-mail: lisarilsr@gmail.com)*

Abstract: In this work, the problem of robustly controlling and monitoring the functioning of an Hydrothermal Carbonization (HTC) batch reactor is addressed. First, the nominal optimal operation is designed by means of dynamical inversion. Then, the application of constructive control with passivity, optimality and detectability notions yields a nonlinear (NL) robust estimator-based output-feedback (OF) tracking optimal controller. From an industrial perspective, the proposed NL OF controller is a control-monitoring (CM) system that tracks the nominal temperature, decides the batch duration, and provides estimates of the physical states and the economic one. The problem is solved within a constructive framework, yielding a CM system design methodology with: (i) systematic construction, (ii) robust functioning, and (iii) a simple tuning scheme. The proposed design is illustrated and tested with a representative example through numerical simulation.

Keywords: Hydrothermal Carbonization, constructive control, nonlinear dynamics, output-feedback control, nonlinear observer, robust stability.

1. INTRODUCTION

In the last decades interest has grown about HTC reactors which appeared as an alternative to produce hydrochar from biomass waste. While the design and monitoring of kinetic and chemical properties (Funke and Ziegler, 2011) has been extensively studied, estimation and control studies are lagging behind. The interaction between control and optimal design leads to integrating models based on control, optimization and numerical analysis theories, including batch (Alvarez et al., 2004) and continuous (González and Alvarez, 2005) process applications. The preceding comments motivate the scope of this work: the development of a non-autonomous finite time joint process-control design methodology for batch HTC reactors which combines NL geometric (Alvarez, 2000), constructive (Sepulchre and Janković, 1997) and optimal (Alvarez et al., 2005) control. Our point of departure is our preliminary feasibility study (Andrade et al., 2020) with emphasis on the construction of the CM system and nominal functioning, without formal robust convergence assessment.

In this work, the problem of robustly controlling and monitoring an Hydrothermal Carbonization (HTC) batch reactor around its *nominal operation* is addressed. The combination of passivity, optimality and detectability tools leads to an estimator-based OF controller that *maximizes the economic profit* of the process. Firstly, the *optimal operation* is designed by means of dynamical inversion (Hirschorn, 1979). Then, an *estimator-based OF controller* which combines a *tracking* and *event* controllers with a *geometric state estimator* is designed. Finally, the robust functioning of the CM system is illustrated with a representative example with numerical simulation.

2. HTC REACTOR AND CONTROL PROBLEM

Consider the reactor of Figure 1 where an exothermic solid-solid carbonization reaction occurs. Wet biomass (M_{bho}) [composed by biomass moisture (M_{ho}) and dry biomass (M_{bo}), hereinafter called biomass] and water (M_{aeo}) are fed. The total amount of water is ($M_{ao} = M_{ho}+M_{aeo}$). The mixture is heated up from an initial to a preset temperature by means of heating steam to degrade the biomass (M_b) in hydrochar (M_c) and water (M_a).

The measurements are: reactor (T) and surrounding (T_s) temperatures, water inflow (W_{ae}), steam outflow (W_{as}) and steam mass flow (W_s) rates. The economic profit (hydrochar minus cost value) per unit time in $[t_o, t_f]$ is (Alvarez et al., 2005; Andrade et al., 2020)

$$J(t) = \frac{c_c M_c(t) - c_M M - c_s \int_{t_o}^{t_f} W_s d_\tau}{t + t_d} - c_o \qquad (1)$$

where c_c and c_M (or c_s) are hydrochar value and raw material (or steam) cost per unit mass respectively, c_o is the operation cost, and t_d is dead time between batches.

From Arrhenius-type carbonization kinetics (Jatzwauck, 2015), three mass balances and an energy balance, and applying theory of reaction networks and stoichiometric invariants, the reactor dynamics consisting of 2 ODEs of: biomass M_b (2a) and temperature T (2b), and 2 algebraic equations of: hydrochar M_c (2d), and water M_a (2e), are given. This system incorporates an economic performance ODE (2c) which state is the batch utility per unit time J (1). The combination of these dynamics results in the following dynamical model (model parameters are shown in table 1):

$$\dot{M}_b = -K(T)M_b := f_\beta,\ M_b(0) = M_{bo},\ t = [t_o, t_f] \qquad (2a)$$

$$\dot{T} = f_T(M_b, T) + h_{T1}(M_b, T)W_{ae} + h_{T2}(M_b, T)W_{as} + h_{T3}(M_b)T_s + g_T(M_b, T)W_s := f_\tau,\ T(0) = T_o \qquad (2b)$$

$$\dot{J} = f_J(M_b, T, J, t) - h_J(t)W_{ae} + g_J(t)W_s := f_{Jd}\,, \qquad J(0) = -\left(\frac{c_M M}{t_d} + c_o\right) := J_o \qquad (2c)$$

$$M_c = -s_c M_b + s_c M_{bo} := f_c \qquad (2d)$$

$$M_a = M_b(s_c - 1) + M - s_c M_{bo} := f_a \qquad (2e)$$

$$y = T \qquad (2f)$$

where

$$\kappa_1 = s_c\kappa_{ac} - \kappa_{ab},\ K(T) = K_0 e^{-\frac{E_a}{R_g T}},$$

$$q(M_b) = \kappa_1 M_b + \kappa_a M - s_c\kappa_{ac}M_{bo} = cp_b M_b + cp_c M_c + cp_a M_a$$

$$f_T(M_b, T) = \frac{-UAT + K(T)(Q_r + \kappa_1 T)M_b}{q(M_b)},$$

$$g_T(M_b, T) = \frac{Q_{v1}(T)}{q(M_b)}\,,\ h_{T1}(M_b, T) = \frac{\kappa_a(T_{ae} - T)}{q(M_b)}$$

$$h_{T2}(M_b, T) = \frac{\kappa_{av}T - Q_{v2}(T)}{q(M_b)}\,,\ h_{T3}(M_b) = \frac{UA}{q(M_b)}$$

$$f_J(M_b, T, J, t) = \frac{1}{t + t_d}\left[-J + c_c s_c K(T)M_b\right],$$

$$g_J(t) = -\frac{c_s}{t + t_d}\,,\ h_J(t) = \frac{c_M}{t + t_d}$$

The *dynamic states* are $\boldsymbol{x} = [M_b, T, J]$. The *quasi-static states* are $\boldsymbol{z} = [M_c, M_a]$. The *measured exogenous inputs* are $\boldsymbol{d} = [T_s, W_{ae}, W_{as}]$, the *control input* is $u = W_s$ and the *measured output* is $y = T$. The parameters are $(\boldsymbol{p}) = [Q_r, s_c, K_o, E_a, M]$. $[t_o, t_f]$ is the *batch duration*. In (2), f_β is the decomposition rate of biomass, $q(M_b)$ is the heat capacity, $f_T(M_b, T)$ is the balance between the heat given

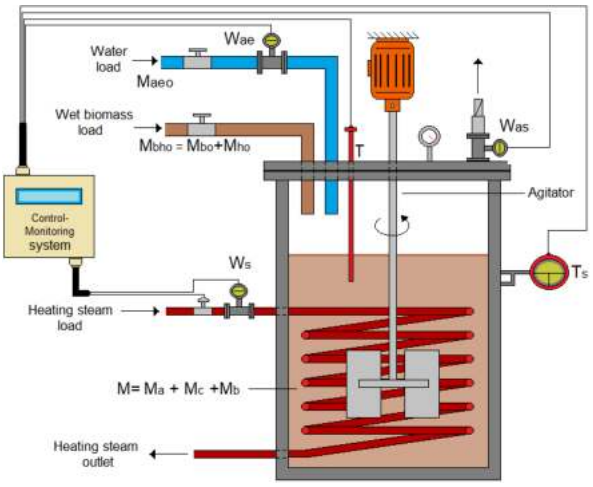

Fig. 1. Hydrothermal Carbonization (HTC) batch reactor

by the carbonization reaction and the heat transferred to the environment, $g_T(M_b, T)$ is the convective heat transfer energy of the heating source, $h_{T1}(M_b, T)$ is the heat exchange between the mixture and water inflow, $h_{T2}(M_b, T)$ is heat extraction through relief valve, and $h_{T3}(M_b)$ is heat transferred by the environment.

In compact vector notation, system (2) is given by

$$\dot{\boldsymbol{x}} = \boldsymbol{f}(\boldsymbol{x}, \boldsymbol{p}, t) + \boldsymbol{H}(\boldsymbol{x}, \boldsymbol{p}, t)\boldsymbol{d} + \boldsymbol{g}(\boldsymbol{x}, \boldsymbol{p}, t)u := \boldsymbol{f_d}(\boldsymbol{x}, \boldsymbol{d}, \boldsymbol{u}, \boldsymbol{p}, t),\ \boldsymbol{x}(0) = \boldsymbol{x_o} \qquad (3a)$$

$$\boldsymbol{z} = \boldsymbol{S}\,\boldsymbol{x} + \boldsymbol{R}(\boldsymbol{p}, \boldsymbol{x_o}),\ y = \boldsymbol{c}\boldsymbol{x}\,,\ t = [t_o, t_f] \qquad (3b)$$

where

$\boldsymbol{x} = [M_b, T, J]'$, $\boldsymbol{z} = [M_c, M_a]'$, $u = W_s > 0$,

$\boldsymbol{d} = [W_{ae}, W_{as}, T_s]$, $\boldsymbol{p} = [Q_r, s_c, K_o, E_a, M]'$, $\boldsymbol{c} = [0, 1, 0]$,

$$\boldsymbol{f}(\boldsymbol{x}, \boldsymbol{p}, t) = \begin{bmatrix} f_\beta(\boldsymbol{x}, \boldsymbol{p}) \\ f_T(\boldsymbol{x}, \boldsymbol{p}) \\ f_J(\boldsymbol{x}, \boldsymbol{p}, t) \end{bmatrix},\ \boldsymbol{g}(\boldsymbol{x}, \boldsymbol{p}, t) = \begin{bmatrix} 0 \\ g_T(\boldsymbol{x}, \boldsymbol{p}) \\ g_J(t) \end{bmatrix},$$

$$\boldsymbol{H}(\boldsymbol{x}, \boldsymbol{p}, t) = \begin{bmatrix} 0 & 0 & 0 \\ h_{T1}(\boldsymbol{x}, \boldsymbol{p}) & h_{T2}(\boldsymbol{x}, \boldsymbol{p}) & h_{T3}(\boldsymbol{x}, \boldsymbol{p}) \\ -h_J(t) & 0 & 0 \end{bmatrix},$$

$\boldsymbol{h_T}(\boldsymbol{x}, \boldsymbol{p}) = [h_{T1}(\boldsymbol{x}, \boldsymbol{p}), h_{T2}(\boldsymbol{x}, \boldsymbol{p}), h_{T3}(\boldsymbol{x}, \boldsymbol{p})]$, $\boldsymbol{c} = [0, 1, 0]$,

$$\boldsymbol{S} = \begin{bmatrix} -s_c & 0 & 0 \\ s_c - 1 & 0 & 0 \end{bmatrix},\ \boldsymbol{R}(\boldsymbol{p}, \boldsymbol{x_o}) = \begin{bmatrix} scM_{bo} \\ M - s_c M_{bo} \end{bmatrix}$$

System (3) is a *non-linear* and *non-autonomous finite time* model, affine in the control input and in the measured exogenous inputs. Since $\boldsymbol{f_d}(\boldsymbol{x}, \boldsymbol{d}, u, \boldsymbol{p}, t)$ is Lipschitz (Elsgotz, 1969) in $[t_o, t_f]$ with respect to the data set $(\boldsymbol{x}, \boldsymbol{d}, u, \boldsymbol{p}, t)$, the unique solution of system (3), for given data $(\boldsymbol{x_o}, \boldsymbol{d}, u, \boldsymbol{p})'$, is the *state motion* $\boldsymbol{x(t)}$ and its respective quasi-static output trajectories $[\boldsymbol{z}(t), y(t)]$

$$\boldsymbol{x}(t) = \boldsymbol{\tau_x}[t, t_o, \boldsymbol{x_o}, d(t), u(t), \boldsymbol{p}], \qquad (4a)$$

$$\boldsymbol{z}(t) = \boldsymbol{\tau_z}[\boldsymbol{x}(t)],\ y(t) = \tau_y[\boldsymbol{x}(t)] \qquad (4b)$$

where $\boldsymbol{\tau_x}$ is the state motion transition map and $\boldsymbol{\tau_z}$ (or τ_y) is the quasi-static (or output measured) transition map.

Consider the nominal data vector: $[\bar{\boldsymbol{x_o}}, \bar{y}, \bar{\boldsymbol{d}}, \bar{\boldsymbol{p}}]'$ which applied to system (3) yields the *nominal operation* (NO)

$$\bar{\boldsymbol{O}} = [\bar{\boldsymbol{x}}(t), \bar{\boldsymbol{z}}(t), \bar{u}(t), \bar{y}(t)],\ t = [t_o, \bar{t_f}] \tag{5}$$

Accord to (3), let us add the error set $(\tilde{\boldsymbol{p}}, \tilde{\boldsymbol{d}}, \tilde{\boldsymbol{u}})$ and noise-like zero-mean state error $(\boldsymbol{\pi})$ generated by faster $(\lambda_\pi >> l_x)$ robust stable parasitic dynamics driven by a fluctuating input $(\boldsymbol{\nu})$, to set the "actual" reactor model

$$\dot{\boldsymbol{\pi}} = \boldsymbol{\gamma}[\boldsymbol{x}, \boldsymbol{d}, u, \boldsymbol{p}; \boldsymbol{\pi}, \boldsymbol{\nu}],\ \boldsymbol{\pi}(0) = \boldsymbol{\pi_o},\ |\nu(t)| \leq \epsilon_\nu^+ \tag{6a}$$

$$\dot{\boldsymbol{x}} = \boldsymbol{f_d}[\boldsymbol{x}, \boldsymbol{d}, u, \boldsymbol{p}, t] + \boldsymbol{e}[\boldsymbol{x}, \boldsymbol{d}, u, \boldsymbol{p}, t; \tilde{\boldsymbol{d}}, \tilde{\boldsymbol{p}}, \boldsymbol{\pi}] \tag{6b}$$

$$\boldsymbol{z} = \boldsymbol{S}\,\boldsymbol{x} + \boldsymbol{R}(\boldsymbol{p}, \boldsymbol{x_o}) + \boldsymbol{h_z}(\boldsymbol{\pi}),\ \boldsymbol{x}(0) = \boldsymbol{x_o} \tag{6c}$$

$$y = \boldsymbol{c}\boldsymbol{x} + h_y(\boldsymbol{\pi}),\ t = [t_o, t_f] \tag{6d}$$

$$\boldsymbol{\gamma}[\boldsymbol{x}, \boldsymbol{d}(t), u(t), \boldsymbol{p}; 0, 0] = \boldsymbol{0},\ \boldsymbol{e}[\boldsymbol{x}, \boldsymbol{d}, u, \boldsymbol{p}, t; 0, 0, 0] = 0$$

$$|\pi(t)| \leq a_\pi e^{-\lambda_\pi} + b_\nu \epsilon_\nu^+$$

The notation $\boldsymbol{m}(\boldsymbol{a}; \boldsymbol{b})$ means that $\boldsymbol{m}$ vanishes with the argument after the semicolon [i.e., $\boldsymbol{m}(\boldsymbol{a}; 0) = 0$]. From now, for simplicity, the explicit dependence on the parameter vector $\boldsymbol{p}$ will be omitted and occasionally used.

2.1 Stability

Since (3) is NL and *non-autonomous*, the standard definitions of stability cannot be used. In batch processes, these definitions applies to a particular *state motion* and its deviations caused by disturbances (Alvarez et al., 2005). For this purpose, let us recall the input-to-state (IS) (Sontag et al., 2004; Isidori, 1995) practical-like (LaSalle and Lefschetz, 1961) non-local stability notion employed before in polymer reactor control and estimation studies (González and Alvarez, 2005; Alvarez, 2000).

Consider the nominal data vector $[\bar{\boldsymbol{x_o}}, \bar{\boldsymbol{d}}, \bar{u}, \bar{\boldsymbol{p}}]'$ that applied to (3) yields the following nominal dynamics

$$\dot{\bar{\boldsymbol{x}}} = \boldsymbol{f_d}[\bar{\boldsymbol{x}}, \bar{\boldsymbol{d}}, \bar{u}, \bar{\boldsymbol{p}}],\ \bar{\boldsymbol{x}}(0) = \bar{\boldsymbol{x_o}},\ t = [t_o, \bar{t_f}] \tag{7}$$

System (7) has unique state motion solution

$$\bar{\boldsymbol{x}}(t) = \boldsymbol{\tau_x}[t, t_o, \bar{\boldsymbol{x_o}}, \bar{\boldsymbol{d}}(t), \bar{u}(t), \bar{\boldsymbol{p}}] \tag{8}$$

For admissibly perturbed data $[\bar{\boldsymbol{x_o}} + \tilde{\boldsymbol{x_o}}, \bar{\boldsymbol{d}} + \tilde{\boldsymbol{d}}, \bar{\boldsymbol{p}} + \tilde{\boldsymbol{p}}]'$ with bounded deviation sizes

$$|\tilde{\boldsymbol{x_o}}| \leq \delta_o,\ |\tilde{\boldsymbol{d}}(t)| := \epsilon_d(t) \leq \epsilon_d^+, |\tilde{\boldsymbol{p}}| \leq \delta_p \tag{9}$$

The motion deviations are

$$\tilde{\boldsymbol{x}}(t) = \boldsymbol{\tau_x}[t, t_o, \bar{\boldsymbol{x_o}} + \tilde{\boldsymbol{x_o}}, \bar{\boldsymbol{d}}(t) + \tilde{\boldsymbol{d}}(t), \bar{\boldsymbol{p}} + \tilde{\boldsymbol{p}}] - \bar{\boldsymbol{x}}(t) \tag{10}$$

Definition 1. The *nominal state motion* (8) over $[t_o, \bar{t_f}]$ is robustly (exponentially) stable if for given deviation sizes (9), the motion deviations (10) are bounded as

$$\begin{aligned} |\tilde{\boldsymbol{x}}(t)| &\leq a_x e^{-l_x(t)}\delta_o + b_p\delta_p + b_d\epsilon_d^+ \\ &\leq a_x\delta_o + b_p\delta_p + b_d\epsilon_d^+ := \epsilon_x(\delta_o, \delta_p, \delta_d^+), \\ &\epsilon_x(0,0,0) = 0,\ (l_x, a_x, b_p, b_d) > 0.\ \bullet \end{aligned} \tag{11}$$

The *nominal state motion* (8) is *non-locally practically* (Hahn, 1967) or *robustly* (V. Lakshmikantham, 1990) stable if admissible and preset disturbance sizes $(\delta_o, \delta_p, \epsilon_d^+)$ produce admissible motion deviation size ϵ_x.

2.2 Control Problem

The design problem consists of: (i) the *nominal operation* (5) with a suitable compromise between profit, control effort, and robustness, and (ii) A CM system (with state $\boldsymbol{x_c}$ made by the estimate state $\hat{\boldsymbol{x}}$ and an integral state $\hat{\imath}$ of a geometric estimator (Álvarez and Fernández, 2009)

$$\dot{\boldsymbol{x_c}} = \boldsymbol{f_c}[\boldsymbol{x_c}, \boldsymbol{d}, y, \bar{y}, u],\ \boldsymbol{x_c}(0) = \boldsymbol{x_{co}}\,, \tag{12a}$$

$$\hat{\boldsymbol{x}} = \boldsymbol{c_e}\boldsymbol{x_c},\ \boldsymbol{x_c} = [\hat{\boldsymbol{x}}, \imath]',\ t = [t_o, t_f] \tag{12b}$$

$$u(t) = \mu[\hat{\boldsymbol{x}}, y, \bar{y}, d],\ t_f = \mu_f[\hat{\boldsymbol{x}}, u(t_f), \boldsymbol{d}(t_f), y(t_f)] \tag{12c}$$

which driven by measured signals $(y, \boldsymbol{d})(t)$ causes the reactor temperature (y) to offsetlessly robustly track $(\bar{y})$, and the state motion $\boldsymbol{x}(t)$ tracks up to admissible deviations the nominal one $\bar{\boldsymbol{x}}(t)$, by adjusting the steam flow rate u, and on the basis of the state estimate $\hat{\boldsymbol{x}}(t)$, determines the batch duration tracks.

3. NOMINAL OPERATION

In this section, the *nominal operation* (5) is designed via iterative dynamical inversion (Hirschorn, 1979) in the sense that for given inverse data $[\boldsymbol{x_{Io}}, \bar{y}(t), \boldsymbol{d}]$, the *nominal state motion-input control* pair $[\boldsymbol{x}(t), u(t)]$ is uniquely-robustly determined.

Take the derivative of (2f) and substitute (2b) to obtain

$$\dot{y} = f_T(M_b, T) + \boldsymbol{h_T}(M_b, T)\boldsymbol{d} + g_T(M_b, T)u \tag{13}$$

whose unique solution for u yields the NL SF control

$$u = \frac{\dot{\bar{y}} - f_T[M_{bI}, \bar{y}] - \boldsymbol{h_T}[M_{bI}, \bar{y}]\boldsymbol{d}}{g_T[M_{bI}, \bar{y}]} := \mu_I[\boldsymbol{x_I}, \boldsymbol{d}, \bar{y}] \tag{14}$$

The heat equation (13) is solvable for u if

$$(Q_{v1}[\bar{y}], q[M_{bI}]) > 0 \Rightarrow g_T[M_{bI}, \bar{y}] = \frac{Q_{v1}[\bar{y}]}{q(M_{bI})} > 0 \tag{15}$$

where $g_T[M_{bI}, \bar{y}] > 0$ is the *relative degree* (RD=1) condition which states that the convective heat transfer energy of the heating source is positive. The application of (14) to system (3) yields the *dynamical inverse* made by the *zero dynamics* (16a) and its *associated control* (16c)

$$\dot{\boldsymbol{x_I}} = \boldsymbol{f_I}\{\boldsymbol{x_I}, \bar{y}, \boldsymbol{d}, \mu_I[\boldsymbol{x_I}, \boldsymbol{d}, \bar{y}]\}, \boldsymbol{x_I} = [M_b, J]' \tag{16a}$$

$$\dot{\bar{y}} = -\lambda_s[\bar{y} - \bar{T}] := f_N,\ \bar{y}(o) = \bar{T}_o \tag{16b}$$

$$u(t) = \mu_I[\boldsymbol{x_I}, \boldsymbol{d}, \bar{y}],\ \boldsymbol{x_I}(0) = \boldsymbol{x_{Io}}, \boldsymbol{f_I} = [f_\beta, f_{Jd}]' \tag{16c}$$

with unique state solution motion

$$\boldsymbol{x_I}(t) = \boldsymbol{\tau_{x_I}}[t, t_o, \boldsymbol{x_{Io}}, \boldsymbol{d}, \bar{y}] \tag{17}$$

The application of the NL control (14) to the reactor (3) yields the nominal operation dynamics, where $f_N : (16b)$

$$\dot{\bar{\boldsymbol{x}}} = \boldsymbol{f_\eta}[\bar{\boldsymbol{x}}, \bar{\boldsymbol{d}}, u, \lambda_s, t],\ \bar{\boldsymbol{x}}(0) = \bar{\boldsymbol{x_o}},\ t = [t_o, \bar{t_f}] \tag{18a}$$

$$\boldsymbol{f_\eta}[\bar{\boldsymbol{x}}, \bar{\boldsymbol{d}}, u, t] = [f_\beta, f_N, f_{Jd}]', [f_\beta, f_{Jd}] : (2a, c). \tag{18b}$$

Since the RD=1 condition (15) is robustly met, the robust stability (passivity) of the nominal state motion (8) must be assessed through numerical simulation. For this aim, apply (14) to the "actual" model (6) to obtain the "actual" nominal dynamics in deviation form with respect to the nominal one (18), consisting of two subsystems: (i) parasitic (19a), and (ii) CL reactor error (19b), dynamics

$$\dot{\boldsymbol{\pi}} = \boldsymbol{\gamma}[\bar{\boldsymbol{x}}, \bar{\boldsymbol{d}}, \bar{u}, \bar{\boldsymbol{p}}; \boldsymbol{\pi}, \boldsymbol{\nu}],\ \pi(0) = \pi_o,\ t = [t_o, \bar{t_f}] \tag{19a}$$

$$\begin{aligned} \dot{\tilde{\boldsymbol{x}}} =& \tilde{\boldsymbol{f}}(\bar{\boldsymbol{x}}, \boldsymbol{p}, t; \tilde{\boldsymbol{p}}) + \tilde{\boldsymbol{H}}(\bar{\boldsymbol{x}}, \boldsymbol{p}, t; \tilde{\boldsymbol{p}})\bar{\boldsymbol{d}} + \tilde{\boldsymbol{g}}(\bar{\boldsymbol{x}}, \boldsymbol{p}, t; \tilde{\boldsymbol{p}})\bar{u} \\ &+ \boldsymbol{\varepsilon}[\bar{\boldsymbol{x}}, \bar{\boldsymbol{d}}, \bar{\boldsymbol{u}}, \boldsymbol{p}, t; \tilde{\boldsymbol{d}}, \tilde{\boldsymbol{u}}, \tilde{\boldsymbol{p}}, \boldsymbol{\pi}],\ \tilde{\boldsymbol{x}}(0) = \tilde{\boldsymbol{x_o}} \end{aligned} \tag{19b}$$

$$\boldsymbol{\varepsilon}[\bar{\boldsymbol{x}},\bar{\boldsymbol{d}},\bar{\boldsymbol{u}},\boldsymbol{p},t;\tilde{\boldsymbol{d}},\tilde{\boldsymbol{u}},\tilde{\boldsymbol{p}},\boldsymbol{\pi}] = \boldsymbol{e}[\bar{\boldsymbol{x}},\bar{\boldsymbol{d}},\bar{\boldsymbol{u}},\boldsymbol{p};\tilde{\boldsymbol{d}},\tilde{\boldsymbol{u}},\tilde{\boldsymbol{p}},\boldsymbol{\pi}] + \boldsymbol{H}(\bar{\boldsymbol{x}},\boldsymbol{p}+\tilde{\boldsymbol{p}},t)\,\tilde{\boldsymbol{d}} + \boldsymbol{g}(\bar{\boldsymbol{x}},\boldsymbol{p}+\tilde{\boldsymbol{p}},t)\,\tilde{u} \quad (19c)$$

where $\boldsymbol{\epsilon}[\bar{\boldsymbol{x}},\bar{\boldsymbol{d}},\bar{\boldsymbol{u}},\boldsymbol{p};\tilde{\boldsymbol{d}},\tilde{\boldsymbol{u}},\tilde{\boldsymbol{p}},\pi]$ is the error caused by deviations on the nominal data vector $[\bar{\boldsymbol{x}},\bar{\boldsymbol{d}},\bar{\boldsymbol{u}},\boldsymbol{p}]$. As we will see in section 5, the state motion (18a) is non-locally robustly practically stable and this behavior is the main objective attainable by any temperature tracking controller.

4. ESTIMATOR-BASED OF CONTROL

In this section, the NL output-feedback (OF) controller (12) is designed along the idea employed before in a batch distillation column (Alvarez et al., 2005).

4.1 State Feedback Control

The enforcement of the output tracking dynamics

$$\dot{e}_y = -k_c[y-\bar{y}],\ e_y(0)=e_{yo},\ e_y(t)=y-\bar{y} \quad (20)$$

to the reactor (3) yields the algebraic equation

$$f_\tau(M_b,y,\boldsymbol{d},u) = \dot{\bar{y}} - k_c[T-\bar{y}] \quad (21)$$

whose unique solution for u yields the NL SF tracking controller [where μ_I is defined in 14]

$$u(t) = \frac{-k_c(y-\bar{y})}{g_T(M_b,y)} - \mu_I(\boldsymbol{x},\boldsymbol{d},y) := \mu[\boldsymbol{x},\boldsymbol{d},y,\bar{y}] \quad (22)$$

The event controller that determines the batch end time (t_f) is derived from the economic state ODE (2c) as

$$t_f = \mu_f[\boldsymbol{x},y(t_f),\boldsymbol{d}(t_f),u(t_f),t_f] \ni f_{Jd}=0 \quad (23)$$

where f_{Jd} (2c) is the batch stop criterion (i.e., $\dot{J}=0$).

4.2 Control-Monitoring (CM) system

The estimation problem consists in infering the unknown dynamic state (M_b, J) and the quasi-static state (M_c, M_a) sets from knowledge of the data set $(\boldsymbol{x_o},\boldsymbol{d},y,u)$. Let us rewrite the reactor model (3) in innovated $(\boldsymbol{x_\iota})$-non-innovated (x_ν) state partitioned form

$$\begin{aligned}\dot{\boldsymbol{x_\iota}} &= \boldsymbol{f_{d\iota}}(\boldsymbol{x_\iota},\boldsymbol{d},u),\ \boldsymbol{x_\iota}(0)=\mathbf{x}_{\iota\boldsymbol{o}},\ t=[t_o,t_f]\\ \boldsymbol{x_\iota} &= [M_b,T]',\ \boldsymbol{x}=[\boldsymbol{x_\iota},x_\nu]'\end{aligned} \quad (24a)$$

$$\dot{x_\nu} = f_{Jd}(\boldsymbol{x_\iota},x_\nu,\boldsymbol{d},u,t),\ x_\nu(0)=x_{\nu o},\ x_\nu = J \quad (24b)$$

$$\boldsymbol{z} = \boldsymbol{S}\,\boldsymbol{x} + \boldsymbol{R}(\boldsymbol{x_o}), y = \boldsymbol{c_\iota x_\iota}, \boldsymbol{c_\iota} = [0\ 1] \quad (24c)$$

The observability map of the innovated state partition is

$$\boldsymbol{o}(\boldsymbol{x_\iota},\boldsymbol{d},u) = [y,\dot{y}]' = [T, f_\tau(\boldsymbol{x_\iota},\boldsymbol{d},u)]',\ f_\tau:(2b) \quad (25)$$

whose Jacobian yields the NL estimation matrix

$$\boldsymbol{O}(\boldsymbol{x_\iota},\boldsymbol{d},u) = \begin{bmatrix} 0 & 1 \\ \dfrac{\partial f_\tau}{\partial M_b} & \dfrac{\partial f_\tau}{\partial T}\end{bmatrix} \quad (26a)$$

$$\begin{aligned}\frac{\partial f_\tau}{\partial M_b} &= \frac{1}{q(M_b)}\left[K(T)(Q_r+k_1T)\right.\\ &\left. -k_1 f_\tau\right] := \frac{f_o(\boldsymbol{x_\iota},\boldsymbol{d},u)}{q(M_b)} := f_\beta^o\end{aligned} \quad (26b)$$

$$\begin{aligned}\frac{\partial f_\tau}{\partial T} &= \frac{1}{q(M_b)}\left\{K(T)M_b\left[\frac{E_a}{R_gT^2}(Q_r+k_1T)+k_1\right]\right.\\ &\left. -UA + k_{av} - \frac{\partial Q_{v2}(T)}{\partial T}W_{as} + \frac{\partial Q_{v1}(T)}{\partial T}u\right\} := f_\tau^o\end{aligned} \quad (26c)$$

The innovated state motion $\boldsymbol{x_\iota}(t)$ is robustly detectable if (26a) is non-singular in $t\in[t_o,t_f]$. Since the heat capacity $q(M_b)$ in (26b) is positive, the next proposition follows.

Proposition 1. The nominal state motion $\bar{\boldsymbol{x}}(t)$ is robustly detectable in $[t_o,t_f]$ if

$$\forall t\in[t_o,t_f] : K(T)\,[Q_r/k_1+T] \neq f_\tau,\ k_1:(2) \quad (27)$$

and $\boldsymbol{x_\nu}(t)$ is robustly stable $\bullet$.

Since the stability of $\boldsymbol{x_\nu}(t)$ follows from the one of the nominal state motion $\bar{\boldsymbol{x}}(t)$ (8), by proposition 1, $\bar{\boldsymbol{x}}(t)$ is: i) robustly observable in $t=[t_o,t_f]-t_e$, where

$$t_e = \mu_e[\boldsymbol{x_\iota},\boldsymbol{d}(t_n),u(t_n),t_n] \ni |f_o(\boldsymbol{x_\iota},\boldsymbol{d},u)| \le \epsilon_e \quad (28a)$$

$$t_s = \mu_s[\boldsymbol{x_\iota},\boldsymbol{d}(t_s),u(t_s),t_s] \ni f_o(\boldsymbol{x_\iota},\boldsymbol{d},u) = 0 \quad (28b)$$

with (t_n) being a short time interval around (t_s) when the algebraic singularity map (26b) $\mathcal{L}_2$ norm is less than a prescribed tolerance (ϵ_e), and ii) almost singular in (t_e). Consequently: (i) $\bar{\boldsymbol{x}}(t)$ is robustly detectable along $[t_o,t_f]$, and (ii) the measurement injection must be applied in $[t_o,t_f]-t_e$ with setting of injection to non-injection mechanism (where P is Heaviside step function)

$$P(t-t_e) = \begin{cases} 0,\ if\ \ |f_o(\boldsymbol{x_\iota},\boldsymbol{d},u)| < \epsilon_e \\ 1,\ if\ \ |f_o(\boldsymbol{x_\iota},\boldsymbol{d},u)| \ge \epsilon_e \end{cases},\ t=[t_o,t_f] \quad (29)$$

The combination of the geometric estimator (30a-c) associated with the detectability property (27), with the tracking (22)-event (23) SF control yields the CM system

$$\begin{aligned}\dot{\hat{\boldsymbol{x}}}_{\boldsymbol{\iota}} =& \boldsymbol{f_{d\iota}}(\boldsymbol{x_\iota},\boldsymbol{d},\mu[\hat{\boldsymbol{x}},\boldsymbol{d},y,\bar{y}]) + P(t-t_e)\\ &\left\{\boldsymbol{O}^{-1}[\hat{\boldsymbol{x_\iota}},\boldsymbol{d},\mu[\hat{\boldsymbol{x}},\boldsymbol{d},y,\bar{y}]](\boldsymbol{k_o}[y-\boldsymbol{c_\iota}\hat{\boldsymbol{x_\iota}}]\right.\\ &\left.+\boldsymbol{\Pi}\hat{\boldsymbol{\iota}})\right\} := \boldsymbol{f_\iota}(\hat{\boldsymbol{x_\iota}},\hat{\iota},\boldsymbol{d},y,\bar{y}),\ \hat{\boldsymbol{x}}_{\boldsymbol{\iota}}(0)=\hat{\boldsymbol{x}}_{\boldsymbol{\iota o}}\end{aligned} \quad (30a)$$

$$\dot{\hat{x_\nu}} = f_{Jd}(\hat{\boldsymbol{x_\iota}},\hat{x_\nu},\boldsymbol{d},\mu[\hat{\boldsymbol{x}},\boldsymbol{d},y,\bar{y}],t),\ \hat{x}_\nu(0)=\hat{x}_{\nu o} \quad (30b)$$

$$\dot{\hat{\iota}} = \omega^3[y-\boldsymbol{c_\iota}\hat{\boldsymbol{x_\iota}}],\ \hat{\boldsymbol{\iota}}(0)=\hat{\boldsymbol{\iota}}_{\boldsymbol{o}},\ \hat{z}=\boldsymbol{S}\hat{\boldsymbol{x}}+\boldsymbol{s} \quad (30c)$$

$$u(t) = \mu[\hat{\boldsymbol{x}},\boldsymbol{d},y,\bar{y}],\ t=[t_o,t_f] \quad (30d)$$

$$t_f = \mu_f[\hat{\boldsymbol{x}},\boldsymbol{d}(t_f),y(t_f),u(t_f),t_f],\ \hat{\boldsymbol{x}}=[\hat{\boldsymbol{x_\iota}},\hat{\boldsymbol{x_\nu}}]' \quad (30e)$$

where

$$\boldsymbol{k_o} = [2\zeta\omega,\omega^2], \boldsymbol{\Pi}=[0,1]', \zeta\in[1,3], \eta\in[5,30], \omega=\eta\omega_n$$

$$\boldsymbol{f_\iota}(\hat{\boldsymbol{x_\iota}},\hat{\iota},\boldsymbol{d},y,\bar{y}) = [f_\beta^\iota,\ f_\tau^\iota]',\ (f_\beta^o,f_\tau^o):(26b,c)$$

$$f_\beta^\iota = f_\beta + P(t-t_e)\left\{(f_\beta^o)^{-1}\left[-2\zeta\omega f_\tau^o+\omega^2\right](T-\hat{T})\right\}$$

$$f_\tau^\iota = \dot{\bar{y}} - k_c[\hat{T}-\bar{y}] + P(t-t_e)\left\{2\zeta\omega(T-\hat{T})+\hat{\iota}\right\}$$

$\hat{\iota}$ is an integral action state that eliminates output mismatch, $\boldsymbol{k_o}$ (or k_ι) is the estimation gain matrix (or integral action gain), η is a speed parameter, ζ is the damping factor, ω_n (or ω) is the natural reactor (or estimator) frequency. The commuter $P(t-t_e)$ ensures the non-local practical convergence, provided the pair $[\zeta,\omega]$ are adequately chosen (Álvarez and Fernández, 2009).

The application of the CM system (30) to (6) yields the "actual" CL dynamics

$$\dot{\boldsymbol{\pi}} = \boldsymbol{\gamma}(\boldsymbol{x}, \boldsymbol{d}; \boldsymbol{\pi}, \boldsymbol{\nu}, \tilde{\boldsymbol{x_\psi}}, \tilde{x_\nu}),\ \boldsymbol{\pi}(0) = \boldsymbol{\pi_o},\ t = [t_o, t_f] \quad (32a)$$

$$\dot{\tilde{\boldsymbol{x_\psi}}} = P(t - t_e)\boldsymbol{A_\psi}(t)\tilde{\boldsymbol{x_\psi}} + \boldsymbol{\varepsilon_\psi}(\boldsymbol{x}, \boldsymbol{d}, \boldsymbol{p}; \tilde{\boldsymbol{x_\psi}}, \tilde{\boldsymbol{d}}, \tilde{\boldsymbol{p}}, \boldsymbol{\pi}),\ \tilde{\boldsymbol{x_\psi}}(0) = \tilde{\boldsymbol{x_{\psi o}}} \quad (32b)$$

$$\dot{\tilde{x_\nu}} = \tilde{f_{Jd}}[\tilde{\boldsymbol{x_\psi}}, \tilde{x_\nu}, \boldsymbol{p}, t] + \varepsilon_\nu(\boldsymbol{x_\psi}, x_\nu, \boldsymbol{d}, \boldsymbol{p}, t; \tilde{\boldsymbol{x_\psi}}, \tilde{x_\nu}, \tilde{\boldsymbol{d}}, \tilde{\boldsymbol{p}}, \boldsymbol{\pi}),\ \tilde{x_\nu}(0) = \tilde{x_{\nu o}} \quad (32c)$$

$$\dot{\boldsymbol{x}} - \dot{\tilde{\boldsymbol{x}}} = \tilde{\boldsymbol{f_d}}[\bar{\boldsymbol{x}}, \bar{y}, \mu(\bar{\boldsymbol{x}}, \bar{y}, \bar{\boldsymbol{d}}; \tilde{\boldsymbol{x}}, \tilde{\boldsymbol{d}}), \tilde{\boldsymbol{d}}, t; \tilde{\boldsymbol{x}}, \tilde{\boldsymbol{d}}, \tilde{\boldsymbol{p}}] + \boldsymbol{\varepsilon_x}(\bar{\boldsymbol{x}}, \bar{y}, \bar{\boldsymbol{d}}, u(t), \bar{\boldsymbol{p}}, t; \tilde{\boldsymbol{x}}, \tilde{\boldsymbol{d}}, \tilde{\boldsymbol{p}}, \boldsymbol{\pi}),\ \tilde{\boldsymbol{x}}(0) = \tilde{\boldsymbol{x}}_{\boldsymbol{o}} \quad (32d)$$

$$\boldsymbol{A_\psi}(t) = \begin{bmatrix} -\boldsymbol{O}^{-1}\{\hat{\boldsymbol{x}}_{\boldsymbol{\iota}}, \boldsymbol{d}, \mu[\hat{\boldsymbol{x}}_{\boldsymbol{\iota}}, \hat{y}, \bar{y}, \boldsymbol{d}]\boldsymbol{k_o} & \boldsymbol{c_\iota} \\ 0 & -\omega^3 \end{bmatrix} \quad (32e)$$

where

$$\tilde{\boldsymbol{x_\psi}} = \hat{\boldsymbol{x_\psi}} - \boldsymbol{x_\psi},\ \boldsymbol{x_\psi} = [\boldsymbol{x_\iota}, \iota]',\ \tilde{x_\nu} = \hat{x_\nu} - x_\nu$$

$$\boldsymbol{\varepsilon_\psi}[\boldsymbol{x}, \boldsymbol{d}, \boldsymbol{p}; \tilde{\boldsymbol{x_\psi}}, \tilde{\boldsymbol{d}}, \tilde{\boldsymbol{p}}, \boldsymbol{\pi}] = \begin{bmatrix} \boldsymbol{\varepsilon_\iota}(\boldsymbol{x_\iota}, \boldsymbol{d}, \boldsymbol{p}; \tilde{\boldsymbol{x}}_{\boldsymbol{\iota}}, \tilde{x_\nu}, \tilde{\boldsymbol{d}}, \tilde{\boldsymbol{p}}, \boldsymbol{\pi}) \\ \omega^3 h_y(\boldsymbol{\pi}) \end{bmatrix}$$

$$\boldsymbol{\varepsilon_\iota}(\boldsymbol{x_\iota}, \boldsymbol{d}, \boldsymbol{p}; \tilde{\boldsymbol{x}}_{\boldsymbol{\iota}}, \tilde{x_\nu}, \tilde{\boldsymbol{d}}, \tilde{\boldsymbol{p}}, \boldsymbol{\pi}) = \tilde{\boldsymbol{f}}_{\boldsymbol{\iota}}[\boldsymbol{x_\iota}, y, \boldsymbol{d}, \boldsymbol{p}; \tilde{\boldsymbol{x}}_{\boldsymbol{\iota}}, \tilde{y}] - \boldsymbol{e_\iota}[\boldsymbol{x_\iota}, \boldsymbol{d}, u(t), \boldsymbol{p}; \tilde{\boldsymbol{d}}, \tilde{\boldsymbol{p}}, \boldsymbol{\pi}] - \boldsymbol{H_\iota}[\boldsymbol{x_\iota}, y, \boldsymbol{p} + \tilde{\boldsymbol{p}}]\tilde{\boldsymbol{d}} - \boldsymbol{g_\iota}(\boldsymbol{x_\iota}, y, \boldsymbol{p} + \tilde{\boldsymbol{p}})\tilde{\mu}[\boldsymbol{x_\iota}, y, \bar{y}, \boldsymbol{d}; \tilde{\boldsymbol{x}}_{\boldsymbol{\iota}}, \tilde{\boldsymbol{d}}]$$

$$\varepsilon_\nu(\boldsymbol{x_\psi}, x_\nu, \boldsymbol{d}, \boldsymbol{p}, t; \tilde{\boldsymbol{x_\psi}}, \tilde{x_\nu}, \tilde{\boldsymbol{d}}, \tilde{\boldsymbol{p}}, \boldsymbol{\pi}) = - e_\nu[\boldsymbol{x_\iota}, x_\nu, \boldsymbol{d}, u(t), \boldsymbol{p}; \tilde{\boldsymbol{d}}, \tilde{\boldsymbol{p}}, \boldsymbol{\pi}] - g_J(t)\tilde{\mu}[\boldsymbol{x_\iota}, y, \bar{y}, \boldsymbol{d}; \tilde{\boldsymbol{x}}_{\boldsymbol{\iota}}, \tilde{\boldsymbol{d}}]$$

$$\boldsymbol{\varepsilon_x}(\bar{\boldsymbol{x}}, \bar{y}, \bar{\boldsymbol{d}}, u, \bar{\boldsymbol{p}}, t; \tilde{\boldsymbol{x}}, \tilde{\boldsymbol{d}}, \tilde{\boldsymbol{p}}, \boldsymbol{\pi}) = \boldsymbol{H}[\bar{\boldsymbol{x}}, \bar{y}, \bar{\boldsymbol{p}} + \tilde{\boldsymbol{p}}, t]\tilde{\boldsymbol{d}} \quad \boldsymbol{e}[\boldsymbol{x}, y, \boldsymbol{d}, u, \boldsymbol{p}; \tilde{\boldsymbol{x}}_{\boldsymbol{\iota}}, \tilde{x_\nu}, \tilde{\boldsymbol{d}}, \tilde{\boldsymbol{p}}, \boldsymbol{\pi}] + \boldsymbol{g}[\bar{\boldsymbol{x}}, \bar{y}, \boldsymbol{p} + \tilde{\boldsymbol{p}}, t]\tilde{u}$$

which has 4 subsystems arranged in fast to slow order: (i) parasitic dynamics (32a), (ii) fast (or slow) estimation dynamics (32b) [or (32c)], and (iii) CL dynamics (32d).

The corresponding robust stability proof can in principle be done with standard (Lyapunov function or small gain) techniques, with emphasis in drawing gain conditions. This task goes beyond the scope of the present study, and here we circumscribe ourselves to verify (in the next section) basic robust functioning features with numerical simulation for the case example.

5. APPLICATION EXAMPLE

Here, the on-line robust functioning of the CM system (30) is tested through numerical simulation of a case example, with $(c_c, c_M, c_s) = [10, 0.1, 2x10^{-6}Q_{v1}(T)](\$/K_g)$, $c_o = 1.1x10^{-3}(\$/s)$ and $t_d = 1800(s)$ (reactor model parameters are listed in Table 1). The third order polynomial function $Q_{v1,2}(T)$ was obtained with regression from the data of latent heat of vaporization of water at saturation pressure between $(273 - 573\,^\circ K)$:

$$f(T) = -2.4x10^{-5}T^3 + 2.3x10^{-2}T^2 - 9,8T + 3958,6 \quad (34)$$

For the execution of robust tests, the "actual": (i) nominal operation (19), and (ii) CL reactor (32), dynamics, were subjected to input disturbances, initial state deviation, and measurement noise. The parasitic dynamics (6a) was emulated with linear oscillators. Both systems were tested with respect to the deviated parameter vector $(\tilde{\boldsymbol{p}})$ as

Table 1. HTC reactor parameters obtained from Libra et al. (2011)*, Jatzwauck (2015)**.

Sym.	Description	Value	Unit
κ_{ab}	Difference between specific heat of liquid water and biomass	2.78	$\frac{KJ}{Kg\,^\circ K}$
κ_{ac}	Difference between specific heat of liquid water and hydrochar	2.92	$\frac{KJ}{Kg\,^\circ K}$
κ_{av}	Difference between specific heat of liquid water and water steam	2.34	$\frac{KJ}{Kg\,^\circ K}$
$Q_v(T)$	Latent heat of vaporization	$f(T)$	$\frac{KJ}{Kg}$
M	Total mass	10000	Kg
U	Heat transport to ambient	2.5	$\frac{W}{^\circ K m^2}$
A	Reactor surface exchange area	19.981	m^2
s_c	Hydrochar stoichiometric coef.	$\frac{72}{162}$	-
Q_r*	Exothermic heat per unit mass	1600	$\frac{KJ}{Kg}$
E_a**	Activation energy	5250	$\frac{KJ}{mol}$
K_o**	Reaction's rate constant	0.1516	$\frac{1}{s}$

$$\tilde{\boldsymbol{p}}^+ = 0.05[Q_r, s_c, K_o, E_a, M],\ |\tilde{\boldsymbol{p}}| \leq \tilde{\boldsymbol{p}}^+. \quad (35)$$

The estimator innovated states (30a) were set with a 5% deviation with respect to their nominal initial values. The biomass (or temperature) *fluctuating input error* e_β (or e_τ) was emulated by a second order linear oscillator with characteristic frequency λ_β (or λ_τ) driven by high-frequency and low-amplitude sinusoidal input ν_β (or ν_τ)

$$\lambda_\beta = 50\lambda_x, \nu_\beta = 20\ sin(0.03t), \boldsymbol{\nu} = [\nu_\beta, \nu_\tau]' \quad (36a)$$

$$\lambda_\tau = 100\lambda_x,\ \nu_\tau = 0.02\ sin(0.06t),\ \boldsymbol{\nu} : (6a) \quad (36b)$$

Steam outflow (d_{ae}) and surrounding temperature (d_s) input disturbances, as well as (zero-mean Gaussian) white noises steam outflow (w_{ae}), surrounding (w_s) and output (w_y) temperature are injected as $[N(0, \sigma_b)$ means zero-mean white noise with standard deviation (σ_b) of $w_b]$

$$d_{ae} = W_a e(t) + \tilde{W}_{ae}(t) + w_{ae} \quad (37a)$$

$$d_s = T_s(t) + \tilde{T}_s(t) + w_s,\ y = T(t) + w_y \quad (37b)$$

$$\tilde{W}_{ae}(t) = 0.001\ sin(0.3t),\ \tilde{T}_s(t) = 0.2\ sin(0.1t) \quad (37c)$$

$$w_{ae} = N(0, \sigma_{ae}), w_s = N(0, \sigma_s), w_y = N(0, \sigma_y) \quad (37d)$$

$$(\sigma_{ae}, \sigma_s, \sigma_y) = (5, 200, 200) \times 10^{-4}. \quad (37e)$$

• *Nominal operation*: The application of control (16a) to (3), with $(\bar{T}, T_o, \lambda_s) = (473, 293, 0.002)$ yields the nominal operation (continuous line) shown in Figure 2 with $\bar{t_f} = 3.6\,h$, where the application of 4 prescribed temperature trajectories (dashed lines) yields the optimal state motion. Its robust stability is enlightened in the sense that temperature and parameter deviations produce admissible state motion deviations $\tilde{\boldsymbol{x}}(t)$.

• *Robust CL behavior*: The application of (30) with $\omega = 0.0064\,s^{-1}$ and $\epsilon_e = 0.015$ yields the CL system (32) with controller-estimator gain triplet $(k_c, \eta, \zeta) = (0.01, 10, 1.5)$ which robust behavior is shown in Figure 3. The results are given: (i) $(t_s, t_f) = (0.8 \pm 0.02, 3.4 \pm 0.24)(h)$ with 6.5% error respect to $\bar{t_f}$, the estimated state motion $\hat{\boldsymbol{x}}(t)$ tends to the nominal one $\bar{\boldsymbol{x}}(t)$ with a bounded (less than 5%) error and the tracking control action results in the measured temperature output $y(t)$ instantly tracking the nominal one $\bar{y}(t)$. The practical results corroborate the

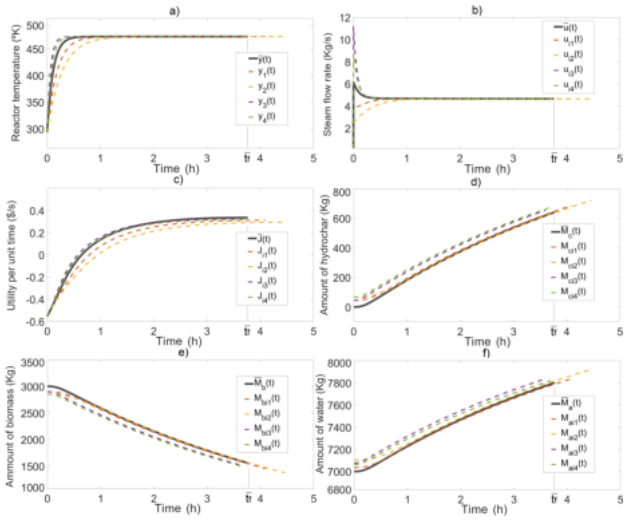

Fig. 2. Robustness of the Nominal operation (continous). (a) Measured output (b) Control effort, (c,e) dynamic states, (d,f) quasi-static states.

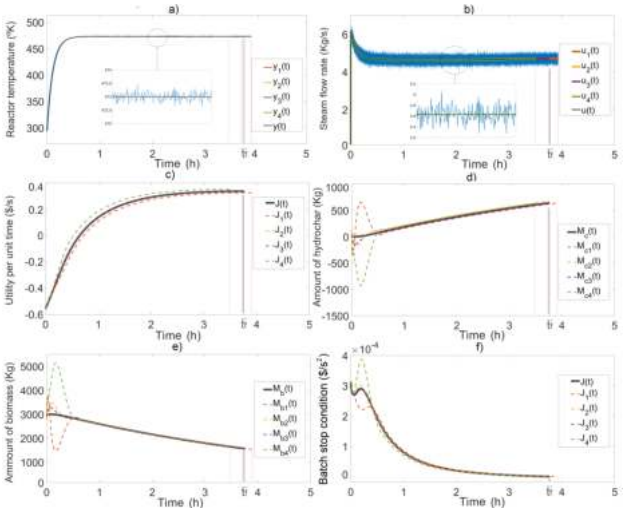

Fig. 3. Robust functioning of the CM system with NL OF controller. (a) Measured output, (b)Control effort, (c,e)dynamic states, (d) quasi-static state, (f) batch stop criterion.

theoretical results, the state motion $\hat{\boldsymbol{x}}(t)$ is non-locally robustly stable with respect to the nominal motion.

6. CONCLUSIONS

The problem of robustly controlling and monitoring a batch HTC reactor has been addressed within a constructive design framework. The resulting CM system has: (i) An optimality and robustness-based nominal offline design scheme, (ii) an optimal-based event controller that decides the batch duration by means of an economic state, (iii) a robust OF controller that tracks the reactor operation along the nominal one, and (iv) a monitoring system that robustly estimates masses of biomass, carbon and water as well as the economic state. Comparing previous results, here the robust functioning of the CM system was formally assessed with a case example through numerical simulation, and solvability with physical meaning was stated on the basis of passivity and detectability of the nominal motion. The proposed design is a point of departure to address: (i) the robust stability proof of the CL system, (ii) multicomponent biomass feed, and (iii) the reactor continuous operation case.

REFERENCES

Alvarez, J. (2000). Nonlinear state estimation with robust convergence. *Journal of Process Control*, 10(1), 59–71.

Alvarez, J., Castellanos-Sahagún, E., Fernandez, C., and Aguirre, S. (2005). Optimal closed-loop operation of binary batch distillation columns. *IFAC Proceedings Volumes*, 16. doi:10.3182/20050703-6-CZ-1902.01676.

Álvarez, J. and Fernández, C. (2009). Geometric estimation of nonlinear process systems. *Journal of process control*, 19(2), 247–260.

Alvarez, J., Zaldo, F., and Oaxaca, G. (2004). Chapter d6 towards a joint process and control design for batch processes. *Computer Aided Chemical Engineering*, 17.

Andrade, S., Alvarez, J., Álvarez Icaza, L., and Samarti, L. (2020). Optimal operation and control of a htc batch reactor. *Memorias del Congreso Nacional de Control Automático 2020*, Número especial 2020.

Elsgotz, L. (1969). *Ecuaciones Diferenciales y calćulo variacional*. Moscu.

Funke, A. and Ziegler, F. (2011). Heat of reaction measurements for hydrothermal carbonization of biomass. *Bioresource Technology*, 102(16), 7595 – 7598.

González, P. and Alvarez, J. (2005). Combined pi inventory control of solution homopolymerization reactors. *Industrial and Engineering Chemistry Research*, 44(18), 7147–7163. doi:10.1021/ie040207r.

Hahn, W. (1967). *Stability of motion*. Springer, Berlin.

Hirschorn, R. (1979). Invertibility of multivariable nonlinear control systems. *IEEE Transactions on Automatic Control*, 24(6), 855–865.

Isidori, A. (1995). *Nonlinear Control Systems*. Communications and Control Engineering. Springer London.

Jatzwauck, M. (2015). Kinetics of hydrothermal carbonization of soft rush. *Biomass and Bioenergy*, 75. doi:10.1016/j.biombioe.2015.02.006.

LaSalle, J. and Lefschetz, S. (1961). *Stability by Liapunov's Direct Method with Applications*. Academic Press, New York, 111 Fifth Avenue.

Libra, J.A., Ro, K.S., Kammann, C., and Funke, A. (2011). Hydrothermal carbonization of biomass residuals. *Biofuels*, 2(1), 71–106. doi:10.4155/bfs.10.81.

Sepulchre, R. and Janković, M. (1997). *Constructive Nonlinear Control*. Communications and Control Engineering. Springer-Verlag London, 1 edition.

Sontag, E., Agachev, A., Utkin, V., and Morse, A. (2004). *Nonlinear and optimal control theory*. Springer, Italy.

V. Lakshmikantham, S. Leela, A.A.M. (1990). *Practical Stability of Nonlinear Systems*. World Scientific.

